Electronic Supplementary Material (ESI) for Physical Chemistry Chemical Physics.

Supporting information

ESIPT-induced Spin-orbit Interactions Enhancement Leads to Tautomer Fluorescence Quenching of the 10-HHBF Molecule

Xin Zhao, Hang Yin*, Wentian Zhang, Jie Guo, Ying Shi*

Institute of Atomic and Molecular Physics, Jilin University, Changchun, 130012, China

**Author to whom correspondence should be addressed:*

yinhang@jlu.edu.cn and shi_ying@jlu.edu.cn

Table of Contents

1. Methods

1.1 Materials

The 10-HHBF molecule was synthesized according to the literature.[1] The tetrahydrofuran (THF) was a super-dry, spectrum-pure, quality reagent purchased from J&K (China) and was used without further purification. The concentration for 10-HHBF in THF was 5×10^{-6} mol/L.

1.2 Quantum chemical calculations

All calculations in our work were performed using the Gaussian 16 package at the B3LYP/TZVP level with the gd3bj dispersion correction.[2-4] Considering the effect brought by THF solvent, the integral equation formalism phase continuum model is adopted in this work.[5] The PySOC program interfaced with Gaussian 16 software was used to calculate the SOC matrix elements.[6] The electron-hole distributions of the singlet and triplet states and the non-radiative decay rates between singlet and triplet states were obtained using Multiwfn software and MOMAP, respectively.[7-9]

1.3 Spectrum measurement

The steady-state absorption was measured on a UV 2550 UV-VIS spectrophotometer (Shimadzu). And fluorescence spectra and excitation spectra were measured with a RF5301 fluorescence spectrophotometer (Shimadzu). Femtosecond Transient absorption spectra were measured with the automated femtosecond transient absorption spectrometer (Helios, Ultrafastsystems), in which details were described in the previous literatures of our research group.[10, 11] Nanosecond TA spectra were acquired on a TA spectrometer (Helios-EOS Fire, Ultrafast System) upon 400 nm excitation. Samples were held in a 2 mm fused silica cuvette.[12-14] ^{1}H NMR and ^{13}C

NMR spectra were measured on a Bruker Avance II 400 spectrometer in deuterated chloroform solution at room temperature with the solvent residual proton signal as a standard. All measurements were performed at room temperature.

2. Aromaticity

To quantitatively compare the aromaticity of excited-state tautomer (Keto* form) for 1-HHBF and 10-HHBF and further support our view that the 10-HHBF occurs the ESIPT reaction, we calculated multicenter bond order and normalized multicenter bond order of the ring related to hydrogen bond. The multicenter bond orders and normalized multicenter bond order of excited-state tautomer for the two molecules are listed in Table S1, and the first row of the Table S1 refers to the adjacent atomic numbers of all atoms in each ring, which corresponds to Fig. S1. For the 1-HHBF, the multicenter bond order of the six-membered ring (18,6,1,9,19,29) with the hydrogen bonding is 0.0012, and that of the ring connected to the ketone group and O-H group is 0.0298 and 0.0528, respectively. For 10-HHBF, the multicenter bond order and normalized multicenter bond order of the ring related to hydrogen bond is close to that for 1-HHBF. That is to say, the aromaticity of the Keto* form for 10-HHBF is comparable with that for 1-HHBF.

Table S1 The multicenter bond order and the normalized multicenter bond order of the ring related to ESIPT process based on the Keto* form in the 1-HHBF (up) and 10-HHBF (down).

	18,6,1,9,19,29	6,5,4,3,2,1	9,1,2,7,8
The multicenter bond order	0.0012	0.0298	0.0528
The normalized multicenter bond order	0.3276	0.5568	0.5553

	2,18,19,3,1,29	17,12,11,10,19,18	19,10,9,4,3
The multicenter bond order	0.0012	0.0171	0.05362
The normalized multicenter bond order	0.3276	0.5569	0.5553

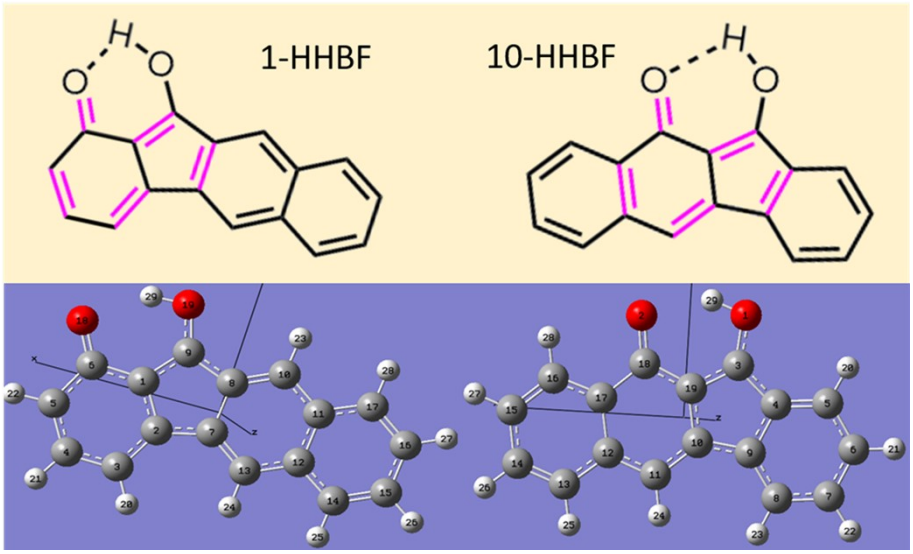

Fig. S1 The excited Keto* form and corresponding atomic number for1-HHBF and 10-HHBF.

3. Emission oscillator strength, Non-Adiabatic Couplings intensity and frontier molecular orbitals

The emission oscillator strength of the Keto* state for 1-HHBF and 10-HHBF is 0.2855 and 0.2872, with little difference, shown in Table S2. And the emission oscillator strength of the Keto* state for 1-HHBF is slightly stronger than that for 10-HHBF, but the 10-HHBF does not show the tautomer fluorescence in contrast to its

isomer 1-HHBF. That reveals that the 10-HHBF has the capability of emitting fluorescence, and thus the luminescent ability is not the reason for quenching of the Keto* state. Beyond that, as we all known, the great overlapping degree for the frontier molecular orbitals (FMOs) between the S_0 and S_1 states is beneficial for the molecule to achieve the fluorescence. Based on that, we also calculated the FMOs from Keto* state to Keto state of 1-HHBF and 10-HHBF, displayed in Fig. S2. Due to the large overlapping degree of HOMO and LUMO of both compounds, they have comparable the ability to emit fluorescence. Therefore, the analysis of FMOs once again demonstrates that luminescent ability is not the reason for the fluorescence quenching of the Keto* form. Moreover, the Non-Adiabatic Couplings (NAC) strength between S_1 and S_0 states for both molecules were listed in Table S2. Obviously, the NAC strength of the 1-HHBF is stronger than that of the 10-HHBF. However, the 10-HHBF does not show the tautomer fluorescence in contrast to its well-known analogue 1-HHBF. That just goes to manifest that the IC process is ruled out as the cause of fluorescence quenching.

Table S2 Calculated the emission oscillator strength and the NAC intensity.

	oscillator strength	NAC ($Bohr^{-1}$)
1-HHBF Keto*	0.2855	4.3005
10-HHBF Keto*	0.2872	4.1604

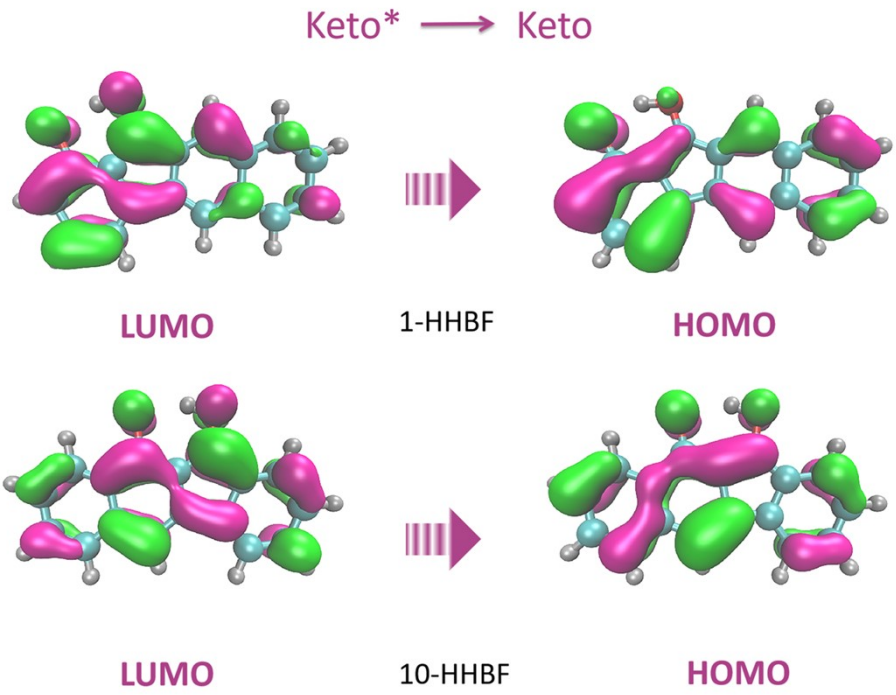

Fig. S2 The HOMO and LUMO of 1-HHBF and 10-HHBF (B3LYP/TZVP/IEFPCM) corresponding to the Keto form and Keto* form.

4. Minimum energy crossing point

Based on the Keto* form, we scanned the PECs of the S_0, S_1 and T_3 states for the 10-HHBF along the rotation coordinate. In the Fig. S3, with the rotation of the hydroxyl group in the Keto* form, we find that the energy level gap of the S_1 and T_3 states become closer proximity. There is a cross point in the S_1 and T_3 states at a rotation coordinate around 80 degree, which is minimum energy crossing point (MECP). Therefore, the rotation of hydroxyl group in the Keto* form can induce the MECP between the S_1 and T_3 states, which is in favor of the occurrence of the ISC process.

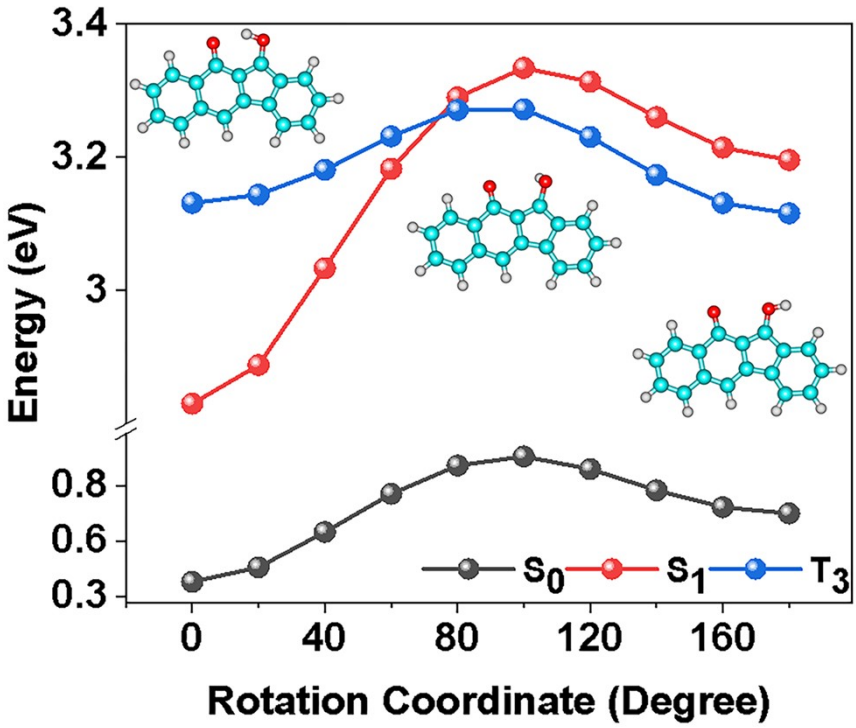

Fig. S3 Calculated the PECs for different electronic states based on the Keto* form of 10-HHBF by fixing the dihedral angle between the hydroxyl group and the deprotonated 10-HHBF molecule.

5. Tautomer fluorescence quenching mechanism

The theoretical and experimental results allow us to gain in-depth understanding of the photochemical behavior of the compound 10-HHBF. Fig. S4 depicts the luminescent mechanism for 10-HHBF. Initially, the 10-HHBF molecule is excited to the S_1 Enol* state under 400 nm light excitation. After excitation, it is followed by the ESIPT process forming the S_1 Keto* structure, with a time scale of about 320 *fs*. Subsequently, the SOC enhancement between S_1 and T_3 states induced by the ESIPT reaction causes the occurrence of the ISC process (11.95 *ps*) between them. Among them, the ESIPT-induced SOC enhancement characteristic for 10-HHBF is attributed to the significant difference in the electron-hole distributions. In addition, the MECP between S_1 and T_3 states can further facilitate the occurrence of the ISC process. Thus,

the emergence of the ESIPT-induced SOC enhancement characteristic and the MECP between the S_1 and T_3 for 10-HHBF provide a reasonable explanation for the fluorescence quenching phenomenon of the Keto* state.

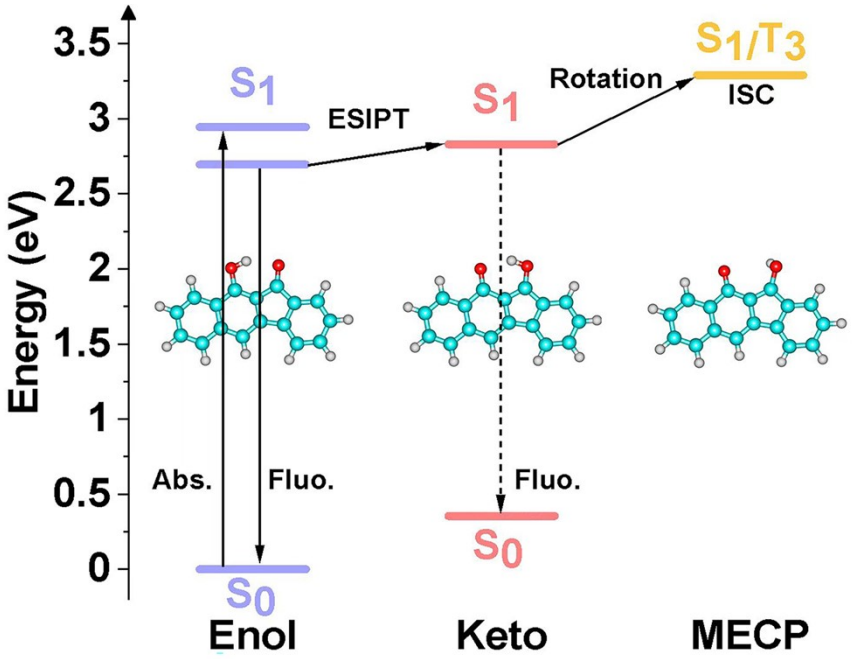

Fig. S4 The schematic diagram of photophysical processes for 10-HHBF in THF solvent.

6. NMR Spectra

^{1}H-NMR spectrum of compound 10-HHBF.

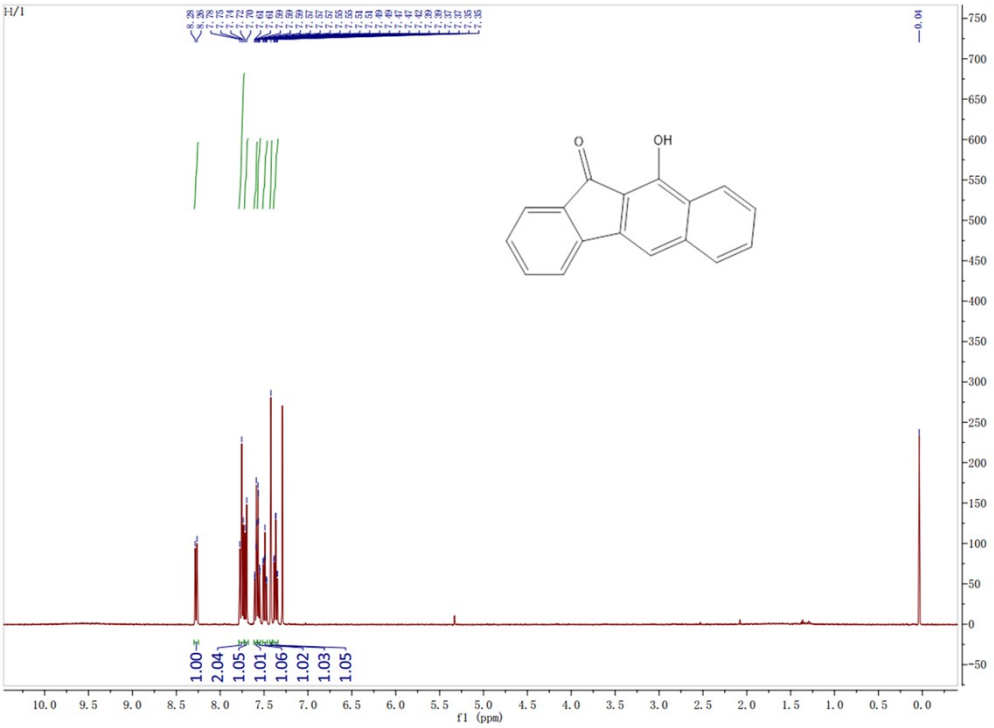

Fig. S5 ^{1}H-NMR spectrum of 10-HHBF in deuterated chloroform. ^{1}H NMR (400 MHz, CDCl3) δ 8.28 (d, J = 8.2 Hz, 1H), 7.78 (t, J = 16.0 Hz, 8.5 Hz, 2H), 7.72 (d, J = 7.7 Hz, 1H), 7.61 - 7.59 (m, 1H), 7.57 - 7.55 (m, 1H), 7.51 - 7.47 (m, 1H), 7.42 (s, 1H), 7.39 - 7.35 (m, 1H).

^{13}C-NMR spectrum of compound 10-HHBF

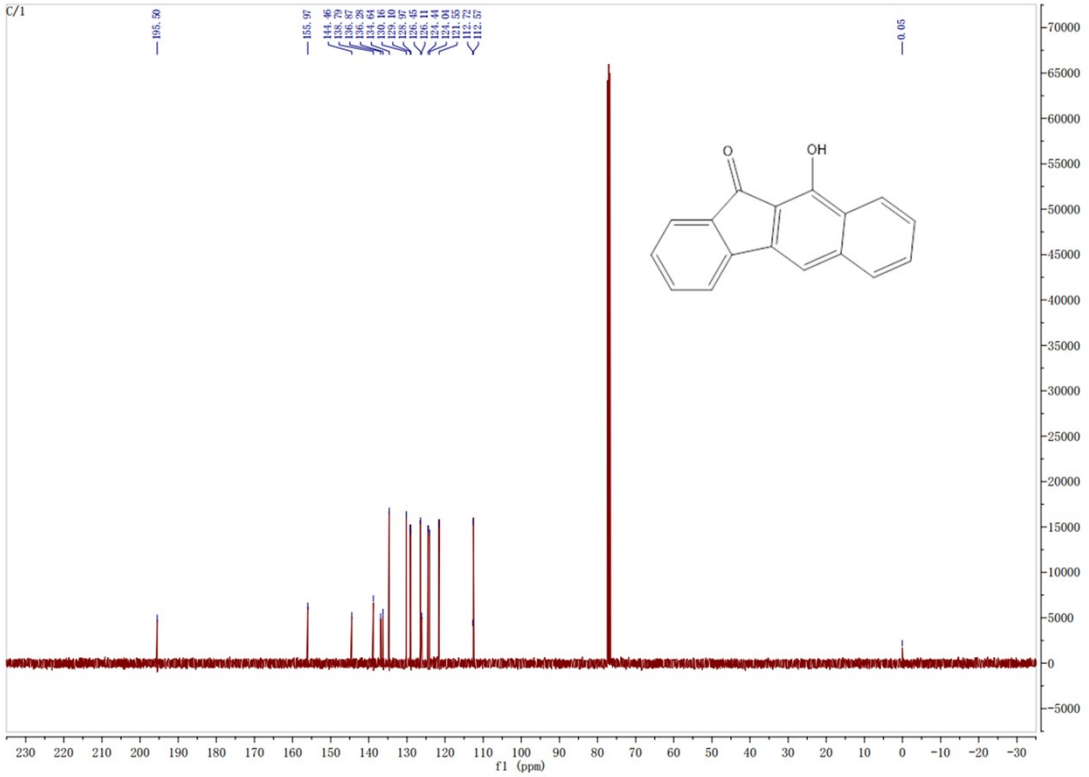

Fig. S6 ^{13}C-NMR spectrum of 10-HHBF in deuterated chloroform. ^{13}C NMR (101 MHz, $CDCl_3$) δ 195.50, 155.97, 144.46, 138.79, 136.87, 136.28, 134.64, 130.16, 129.10, 128.97, 126.45, 126.11, 124.44, 124.04, 121.55, 112.72, 112.57.

7. Nanosecond transient absorption spectroscopy

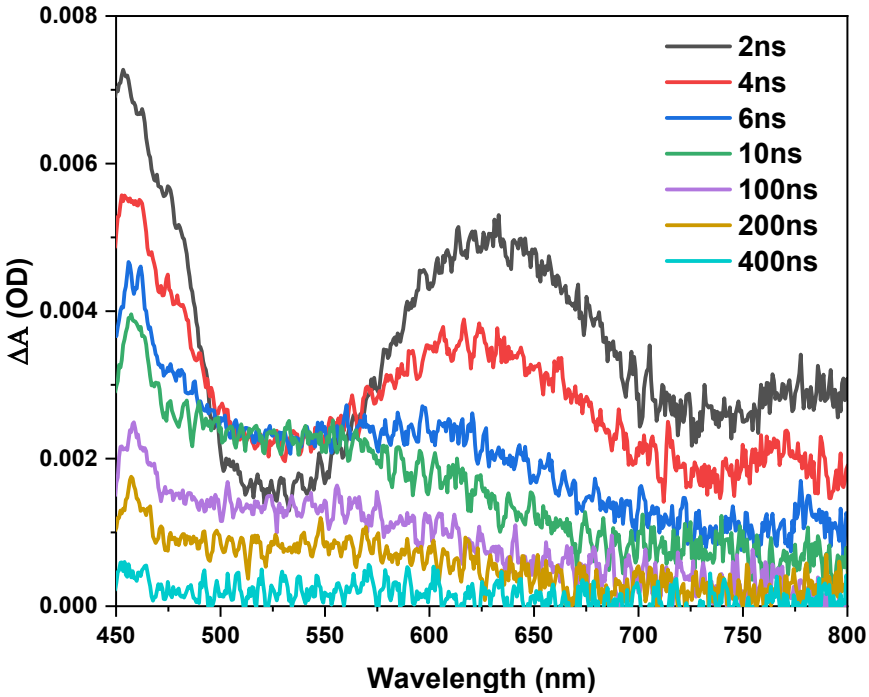

Fig. S7 Nanosecond transient absorption spectra recorded for 10-HHBF in THF between 2 *ns* and 400 *ns* after excitation at 400 nm.

8. Absorption and fluorescence spectroscopy

As shown in Fig. S8 (b), we only observe the S_1 Enol* form emission for 10-HHBF at around 500 nm under different solution concentrations, while the S_1 Keto* form emission is not observed. Moreover, according to Fig. S8 (c), in the concentration range from 5×10^{-6} mol/L to 1×10^{-4} mol/L, the fluorescence peak intensity of the 10-HHBF demonstrates a direct proportionality to the concentration of the solution. As a result, in the concentration range from 5×10^{-6} mol/L to 1×10^{-4} mol/L, the aggregate effect in the femtosecond TA measurement for 10-HHBF is excluded. In conclusion, In conclusion, given that we do not observe the S_1 Keto* emission of 10-HHBF across different concentrations, and considering the fact that the concentration of 10-HHBF in THF in our femtosecond TA measurement is $5 \times 10^{-}$

^{6} mol/L, we can confidently exclude the aggregate effect in our femtosecond TA measurement.

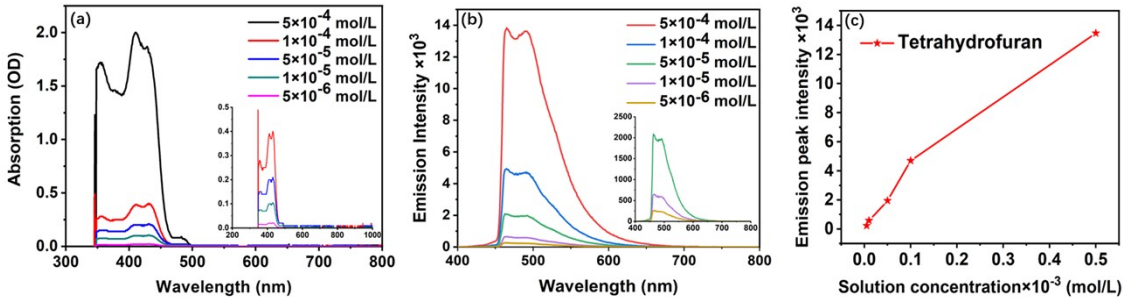

Fig. S8 The absorption (a) and fluorescence (b) spectra of the 10-HHBF under different concentration. The change of the fluorescence peak intensity under different solution concentrations (c).

9. Reference

[1] J. Piechowska, G. Angulo, Frustrated excited state intramolecular proton transfer (ESIPT) in 10-hydroxy-11*H*-benzo[*b*]fluoren-11-one: Synthesis and photophysics, Dyes Pigments, 2019, 165, 346-353. DOI: 10.1016/j.dyepig.2019.02.031

[2] M. J. Frisch, G. W. Trucks, H. B. Schlegel, G. E. Scuseria, M. A. Robb, J. R. Cheeseman, et al. Gaussian 16 Rev, B.01, Wallingford, CT, USA: Gaussian, Inc, 2016.

[3] A. Schäfer; C. Huber; R. Ahlrichs, Fully optimized contracted Gaussian basis sets of triple zeta valence quality for atoms Li to Kr, 1994, 100, 5829–5835. DOI: 10.1063/1.467146

[4] S. Grimme, J. Antony, S. Ehrlich, H. Krieg, A consistent and accurate ab initio parametrization of density functional dispersion correction (DFT-D) for the 94 elements H-Pu, J Chem Phys, 2010, 132, 154104. DOI: 10.1063/1.3382344

[5] R. Cammi, J. Tomasi, Remarks on the use of the apparent surface charges (ASC) methods in solvation problems: Iterative versus matrix-inversion procedures and the renormalization of the apparent charges, J Comput Chem, 1995, 16, 1449-1458. DOI: 10.1002/jcc.540161202

[6] X. Gao, S. Bai, D. Fazzi, T. Niehaus, M. Barbatti, W. Thiel, Evaluation of Spin-Orbit Couplings with Linear-Response Time-Dependent Density Functional Methods, J Chem Theory Comput, 2017, 13, 515-524. DOI: 10.1021/acs.jctc.6b00915

[7] T. Lu, F. Chen, Multiwfn: A multifunctional wavefunction analyzer, J Comput Chem, 2012, 33, 580-592. DOI: 10.1002/jcc.22885

[8] Q, Peng, Y. P. Yi, Z. G. Shuai, J. S. Shao, Toward Quantitative Prediction of Molecular Fluorescence Quantum Efficiency: Role of Duschinsky Rotation, J Am Chem Soc, 2007, 129, 9333-9339. DOI: 10.1021/ja067946e

[9] Z. G. Shuai, Thermal Vibration Correlation Function Formalism for Molecular Excited State Decay Rates, Chin J Chem, 2020, 38, 1223-1232. DOI: 10.1002/jcc.22885

[10] H. Yin, Y. M. Zhang, H. F. Zhao, G. J. Yang, Y. Shi, S. X. A. Zhang, D. J. Ding, Optical

anti-counterfeiting of a single molecule by two solvents based on intra- and intermocular excited state proton transfer mechanisms, Dyes Pigments, 2018, 159, 506-512. DOI: 10.1016/j.dyepig.2018.07.032

[11] H. Li, J. H. Han, H. F. Zhao, X. C. Liu, Y. Luo, Y. Shi, C. L. Liu, M. X. Jin, D. J. Ding, Lighting Up the Invisible Twisted Intramolecular Charge Transfer State by High Pressure, J Phys Chem Lett, 2019, 10, 748–753. DOI: 10.1021/acs.jpclett.9b00026

[12] Y. Y. Liu, H. F. Pan, J. H. Xu, , J. Q. Chen, Long Chain Fatty Acid Affects Excited State Branching in Bilirubin-Human Serum Protein Complex. Chin. J. Chem. Phys. 2021, 34, 621-627. DOI: 10.1063/1674-0068/cjcp2012220

[13] Z. Chen, Y. Y. Liu, X. X. He, J. Q. Chen, Ultrafast Excited State Dynamics of Biliverdin Dimethyl Ester Coordinate with Zinc Ions. Chin. J. Chem. Phys. 2020, 33, 69-74. DOI: 10.1063/1674-0068/cjcp1911193

[14] Li. X, Wang. X, Lv. M, Zhou. Z, Pan. H, Chen. J, Direct Observation of a Singlet ππ* and nπ* Equilibrium State in 2-Amino1,3,5-Trainzine Solution. Chin. J. Chem. Phys. 2022, 35, 747-753. DOI: 10.1063/1674-0068/cjcp2202029